Journal of Magnetism and Magnetic Materials 469 (2019) 391–397

Contents lists available at ScienceDirect

Journal of Magnetism and Magnetic Materials

journal homepage: www.elsevier.com/locate/jmmm

Research articles

Co_2W hexaferrite nanoparticles-carbon nanotube microwave absorbing nanocomposite

Ali Ghasemi*, Gholam Reza Gordani, Ebrahim Ghasemi

Materials Engineering Department, Malek Ashtar University of Technology, Shahin Shahr, Iran

ARTICLE INFO

Keywords:
Hexaferrite
Carbon nanotubes
Nanocomposites
Magnetic properties

ABSTRACT

Co_2W-type hexaferrite nanoparticles with composition of $SrCo_{2-x}(MnZnCa)_{x/3}Fe_{16}O_{27}$(x = 0–0.5) were synthesized by a co-precipitation method. The synthesized nanoparticles were decorated on the outer surface of multi-walled carbon nanotubes by chemical method. X-ray diffractometry, scanning electron microscopy, vibrating sample magnetometry, magnetic susceptometer and vector network analyzer were utilized to characterize the structural, magnetic, and reflection loss properties of the nanocomposites. The structural results showed a perfect diffusion of Mn, Zn and Ca ions into the crystal structure of Co_2W hexaferrite without forming any secondary phases. The SEM images provide clear information about the size of nanoparticles (50–85 nm) through these samples. The hysteresis loops showed hard magnetic property with enhanced coercivity which reflects that the synthesized particles have almost high magnetic anisotropic field, well suitable for absorbing materials. The coercivity (H_c) increased from 1450 Oe at $x = 0.0$, to 1650 Oe at $x = 0.3$, and then decreases to 1320 Oe at $x = 0.5$. High reduction in the coercivity was detected consistent with the large particle sizes for these samples. Ferrite nanoparticles were decorated on the surface of carbon nanotubes in almost constant distance. The interacting mode was confirmed between magnetic nanoparticles by means of plotting real and imaginary parts of magnetic susceptibility versus temperature at various frequencies. Based on reflectivity measurement, the sample with $x = 0.3$ showed a maximum reflection loss of −37 dB at the frequency of 9.4 GHz. This sample revealed the best performance with low reflectivity and high absorption broadband (4 GHz) at X-band frequency range.

1. Introduction

In recent years, increasing the need for anti-electromagnetic interference coatings to prevent electromagnetic pollution and also to enrich the field of stealth technology, has led to an increase in studies on materials capable of absorbing electromagnetic waves [1,2]. Two fundamental conditions are essential for materials which suitable for these applications, the first is impedance matching characteristic and the second is attenuation characteristic.

M-type and W-type hexaferrites are the new types of microwave absorbents developed [3]. Due to the great permeability, high value of magnetization, planar anisotropic behavior, and good dielectric properties at microwave frequencies, the W-type hexaferrites are suitable for electromagnetic interference suppression and radar absorbent materials (RAM) [4,5]. Ideally, good microwave absorbents possess a low reflection loss, wide absorption bandwidth, and low matching thickness. However, practically, there exists no material able to fulfill all these requirements [6].

The crystal structure of W-type hexagonal ferrite is very complex and consist of two block of R and S (where R is hexagonal and S is cubic spinel). There are seven non-equivalent sub-lattices in the W-type hexaferrites where cations can occupy, i.e. 12k, 4fVI, 6g, 4f (octahedral), 4e, 4fIV (tetrahedral) and 2d (bipyramidal) [7].

A study on divalent ions substituted W-type hexagonal ferrite has reported minimum reflection losses reaching −35 dB but with a narrow absorption bandwidth less than 2 GHz [8]. The Previous literatures revealed a considerable modification of the W-type ferrite based on the replacement of metal ions [9–11].

For example, it has been reported that magnetic saturation and coercivity of W-type hexaferrite decreased with an increase in cobalt substitution [12]. Of course this depends on the production method. It is also inferred that the Zn substitution for Co at a suitable proportion may enhance saturation magnetization resulting in the thinner and superior microwave absorbents in terms of bandwidth and reflection losses [13]. Considering the outstanding properties of CNTs as well as strontium ferrite nanoparticles, SrM/CNTs nanocomposites would be

* Corresponding author.
E-mail address: Ali13912001@yahoo.com (A. Ghasemi).

https://doi.org/10.1016/j.jmmm.2018.09.010
Received 29 April 2018; Received in revised form 19 August 2018; Accepted 4 September 2018
Available online 05 September 2018
0304-8853/

very attractive for practical applications. Strontium ferrite/CNTs can be used in the fabrication of high frequency microwave absorbing nanocomposite, and various microwave and radar devices due to its high permeability and permittivity losses. Moreover, the exceptional electronic properties and the hollow structure characteristic of CNTs could have an important potential for the use of magnetic nanotubes in many other applications ranging from electromagnetic devices to magnetically guided drug delivery systems.

In current research, the magnetic properties and microwave-absorbing characteristic of single-layer Zn, Mn and Ca substituted Co_2W hexaferrite- carbon nanotubes are evaluated. Carbon nanotubes were employed in order to match the permeability and permittivity of nanocomposites. The correlation between structural features and magnetic consequences were carried out. The phenomenological rules of Neel-Brown and Vogel-Fulcher were employed to evaluate the existence of magnetic interaction between nanoparticles. Reflection loss evaluations indicated that the samples display a great potential application as wide-band electromagnetic wave absorbers.

2. Materials and methods

W-type hexaferrite with nominal composition of $SrCo_{2-x}(MnZnCa)_{x/3}Fe_{16}O_{27}$ (x = 0–0.5) was synthesized by a co-precipitation method. High purity raw materials including $FeCl_3{\cdot}6H_2O$, $SrCl_2{\cdot}6H_2O$, $CoCl_2{\cdot}4H_2O$, $ZnCl_2$, $MnCl_2{\cdot}4H_2O$, $CaCl_2{\cdot}2H_2O$ and NaOH were employed for the synthesis process. Stoichiometry amounts of the metal salts were separately dissolved in distilled water and then mixed in a beaker to form a homogeneous solution. Drop-wise addition of sodium hydroxide was performed under constant stirring at ambient temperature until the solution pH reached 11. The precipitates were washed several times with distilled water. Afterwards, the product was dried at 110 °C, and was ground using a mortar and a pestle. Finally, the dried powder was calcined at 1100 °C for 3 h. The nanocomposites were synthesized by chemical method. In the second step, the carbon nanotubes were functionalized in nitric acids for 7 h. Then, the MWCNTs were dispersed in ethylene chloride solution by employing high power ultrasonic for 90 min, and the pH value was kept at 9.5. In the following step, the carbon nanotube solution was dripped to ferrite solution with ultrasonication. The CNTs were added with 5 vol% to SrM solution in order to evaluate the effect of CNTs on magnetic properties of nanocomposites.

The phase compositions of the samples were identified by XRD (Phillips X' Pert PRO 3040/60, *Cu*-Kα radiations). Microstructural investigations were conducted by scanning electron microscopy (Hitachi S-3400N). The magnetic parameters were measured at room temperature using vibrating sample magnetometer at maximum field strength of 10 kOe. Magnetic susceptibility was measured by magneto-susceptometer lake shore model 7000. The real and imaginary parts of effective magnetic susceptibility were measured at various frequencies versus temperature. The type of interaction between nanoparticles was carried out by comparison of Neel-Brown and Vogel-Fulcher models. After preparation of nanocomposites the absorbing specimens were made by mixing nanocomposite and PVC powder in the mass ratio of 70:30. The pressed composites were in the cylindrical form with the thicknesses of 1.5 mm and the diameter of 40 mm. Reflection loss variation (in *dB*) versus frequency within the range of 8–12 GHz was investigated by an HP 8722ETvector network analyzer.

3. Results and discussion

3.1. Structural and morphology characteristics

Fig. 1 shows the XRD patterns of $SrCo_{2-x}(MnZnCa)_{x/3}Fe_{16}O_{27}$ particles with different cation contents (x = 0.0–0.5). It is observed that the single phase W-type hexaferrite with no secondary impurity phases was formed. The crystal structures of W-type hexaferrites perfectly

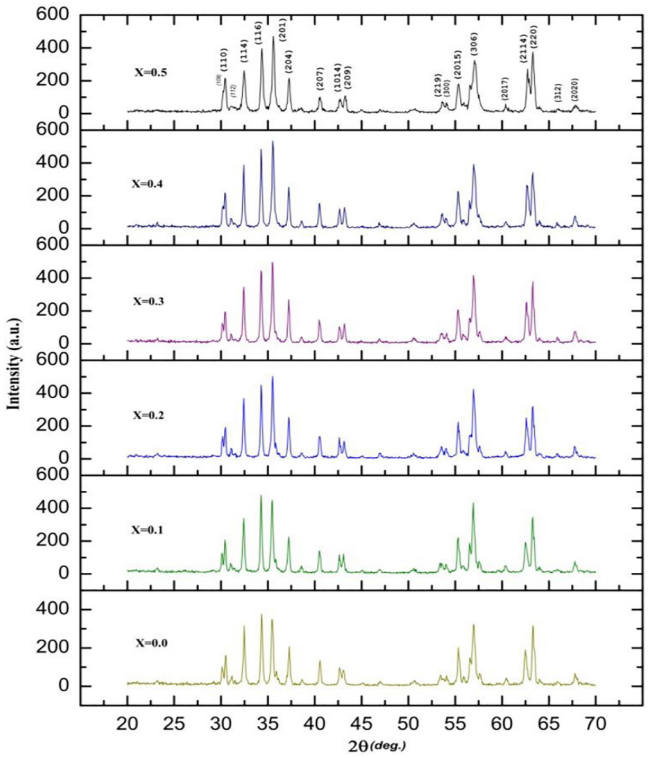

Fig. 1. XRD patterns of substituted $SrCo_{2-x}(Mn_xZn_xCa_x)_{1/3}Fe_{16}O_{27}$(x = 0.0–0.5) hexaferrites.

match with the standard patterns of pure Co_2W (PDF N0. 01-078-0135). It is indicated that the Mn, Zn and Ca ions were completely solved into the hexaferrite crystal lattice. The lattice parameters *a*(Å), *c*(Å) and unit cell volume (V_{cell}) were calculated based on XRD patterns using Eqs. (1) and (2). The values acquired for such parameters are listed in Table 1, which were well consistent with the Co_2-W hexaferrite lattice parameters reported by Stergiou C et al. [14].

$$\frac{1}{d_{hkl}^2} = \frac{4(h^2 + kh + k^2)}{3a^2} + \frac{l^2}{c^2} \quad (1)$$

$$V_{cell} = a^2 c \sin 120° \quad (2)$$

where *d* is the space between the crystalline planes and *h*, *k* and *l* are the corresponding Miller indices. The average crystallite size of Co_2W hexaferrite nanoparticles synthesized at different content of substituted metallic ions was calculated from the XRD data using the Scherrer equation. It was observed that, with an increase in concentration of metallic ions, the crystallite size increased from 50 nm (for $x = 0$) to the 85 nm (for $x = 0.5$).

Crystal structure of Co_2W ferrites is hexagonal. Therefore, magneto-crystalline anisotropy can be one of the main characteristics of these ferrites because of that the c-axis is the easy axis in Co_2W hexaferrites. Subsequently, there is noticeable variation in parameter *c* than *a* with increasing of dopant cations content in crystal structure of hexaferrites.

Table 1
Parameters obtained by XRD, VSM and RL results for $SrCo_{2-x}(Mn_xZn_xCa_x)_{1/3}Fe_{16}O_{27}$ (x = 0–0.5).

Sample	*a* (Å)	*c* (Å)	V_{cell} (Å^3)
x = 0.0	5.917	32.663	1143
x = 0.1	5.923	32.691	1147
x = 0.2	5.929	32.715	1150
x = 0.3	5.930	32.733	1151
x = 0.4	5.934	32.770	1154
x = 0.5	5.936	32.793	1156